## Short Communication

Correspondence
H. Adler
h.adler@helmholtz-muenchen.de

Received 9 January 2012 Accepted 16 January 2012

## ORF23 of murine gammaherpesvirus 68 is non-essential for *in vitro* and *in vivo* infection

S. Ohno,† B. Steer, C. Sattler and H. Adler

Institute of Molecular Immunology, Helmholtz Zentrum München – German Research Center for Environmental Health, Munich, Germany

Although ORF23 is conserved among gammaherpesviruses, its role during infection is unknown. Here, we studied the expression of ORF23 of murine gammaherpesvirus 68 (MHV-68) and its role during infection. ORF23 mRNA was detected in infected cells as a late transcript. The ORF23 protein product could be expressed and detected as an N-terminally FLAG-tagged protein by Western blot and indirect immunofluorescence. To investigate the role of ORF23 in the infection cycle of a gammaherpesvirus, we constructed an ORF23 deletion mutant of MHV-68. The analysis of the ORF23 deletion mutant suggested that ORF23 of MHV-68 is neither essential for replication in cell culture nor for lytic or latent infection *in vivo*. A phenotype of the ORF23 deletion mutant, reflected by a moderate reduction in lytic replication and latency amplification, was only detectable in the face of direct competition to the parental virus.

Murine gammaherpesvirus 68 (MHV-68) is a member of the gammaherpesviruses and closely related to the human gammaherpesviruses Kaposi's sarcoma-associated herpesvirus (KSHV) and Epstein-Barr virus (EBV) (Virgin et al., 1997). MHV-68 serves as a small animal model to investigate gammaherpesvirus pathogenesis (Barton et al., 2011; Blackman & Flaño, 2002; Nash et al., 2001; Simas & Efstathiou, 1998; Speck & Virgin, 1999; Virgin & Speck, 1999). The nucleotide sequence of MHV-68 is similar to EBV and even more closely related to KSHV (Virgin et al., 1997). In addition to virus-specific genes, MHV-68 contains genes that are homologous to cellular genes or to genes of other gammaherpesviruses. One of the latter is ORF23. Although being conserved among gammaherpesviruses, the function of ORF23 is unknown. Here, we studied the expression of ORF23 of MHV-68 and explored an ORF23 deletion mutant to investigate the role of ORF23 in the infection cycle of a gammaherpesvirus.

To analyse the expression of ORF23 at the mRNA level, the persistently infected cell line S11 (Usherwood *et al.*, 1996) was treated with 20 ng 12-*O*-tetradecanoyl-phorbol-13-acetate (TPA) ml<sup>-1</sup> to induce the lytic cycle, and expression of ORF23 was examined by real-time RT-PCR. Expression of ORF23 mRNA was readily inducible by TPA stimulation (Fig. 1a). In addition, we analysed the expression of ORF23 mRNA after infection of NIH3T3 cells in the presence or absence of either the protein synthesis inhibitor cycloheximide (CHX; 10 μg ml<sup>-1</sup>) or the DNA synthesis inhibitor phosphonoacetic acid (PAA;

†Present address: Department of Virology, Faculty of Medicine, Kyushu University, Fukuoka 812-8582, Japan.

Supplementary material is available with the online version of this paper.

200 μg ml<sup>-1</sup>). Treatment with CHX or PAA strongly reduced expression of ORF23 mRNA and thus allowing classification as a late transcript (data not shown). Next, we wanted to analyse the expression and intracellular localization of ORF23 at the protein level. For this purpose, the predicted ORF (Virgin et al., 1997) was cloned as an N-terminally FLAG-tagged protein into the eukaryotic expression vector pCA7, a derivative of pCAGGS (Niwa et al., 1991). After transient transfection, expression of the FLAG-tagged ORF23 protein (FLAG-ORF23) could be demonstrated both by Western blot (Fig. 1b) and by immunofluorescence microscopy (Fig. 1c) by using an anti-FLAG antibody. In immunofluorescence analysis, the protein displayed both a nuclear and a cytoplasmic localization with a dotted pattern. To test whether the presence of additional viral proteins might change the localization of the ORF23 protein, cells were transiently transfected with plasmid DNA and simultaneously infected with BAC-derived, GFP-expressing MHV-68. The localization of the ORF23 protein did not change after infection (Fig. 1d).

To investigate the role of ORF23 in the infection cycle, we constructed an ORF23 deletion mutant ( $\Delta$ 23) with a deletion of nucleotides 37 226–37 766 [Fig. S1(a) and Supplementary Methods, available in JGV Online]. To exclude the possibility that a potential phenotype of the ORF23 deletion mutant might be due to rearrangements outside the mutated region, a revertant (23R) of the ORF23 deletion mutant was also generated. The BAC-cloned genomes were analysed by restriction enzyme analysis with several restriction enzymes [Fig. S1(b)]. Viruses were reconstituted and the BAC cassette was removed as described previously (Adler *et al.*, 2000). The genomes of

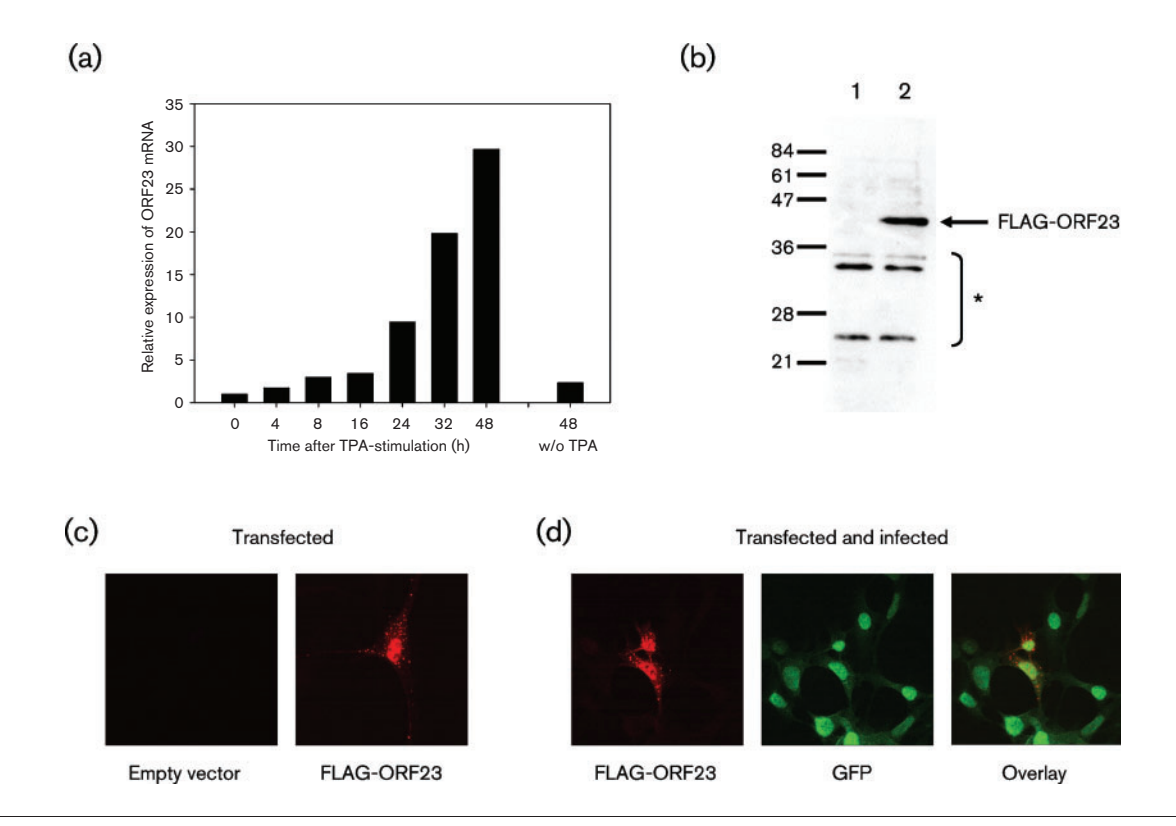


**Fig. 1.** Expression of ORF23 mRNA and protein. (a) Expression of ORF23 mRNA. S11 cells were treated with 20 ng TPA ml<sup>-1</sup> and expression of ORF23 was examined by real-time RT-PCR. The results were normalized to the expression of the cellular gene L8 and are depicted as expression relative to the value obtained at 0 h after TPA stimulation, which was set to 1. One representative out of three independent experiments is shown. (b) Detection of ORF23 protein by Western blot analysis. The coding sequence of ORF23 was cloned with an N-terminal FLAG-tag into the eukaryotic expression vector pCA7. HEK293T cells were transfected with either the empty vector (lane 1) or the FLAG-ORF23 encoding vector (lane 2). Twenty-four hours after transfection, expression of ORF23 was detected by Western blot analysis. Marker sizes (kDa) are indicated on the left. The arrow indicates FLAG-ORF23 protein of the expected size (approx. 43.5 kDa). The asterisk marks unspecific bands that can be taken as control for equal loading. (c) Detection of ORF23 protein by immunofluorescence. NIH3T3 cells were transfected with either the empty vector (left panel) or the FLAG-ORF23 encoding vector (right panel). Twenty-four hours after transfection, protein expression was detected by immunofluorescence microscopy. (d) As in (c), but cells were also infected with BAC-derived, GFP-expressing MHV-68. Staining for FLAG-ORF23 protein expression is shown in the left panel and expression of GFP as infection marker is shown in the middle panel. The right panel depicts the resulting overlay. The images in (c) and (d) were acquired at a 1000-fold magnification.

the reconstituted viruses were also analysed by restriction enzyme and Southern blot analyses [Fig. S1(c)].

Transfection of the ORF23 mutant BAC plasmid into BHK-21 cells led to the development of plaques, indicating that ORF23 is not essential for lytic replication *in vitro* (data not shown). This is consistent with earlier findings by others (Song *et al.*, 2005). To determine the *in vitro* growth kinetics of the recombinant viruses, multi-step growth curves were performed in two different murine cell lines, NIH3T3 (fibroblasts) [Fig. S2(a–c)] and MLE-12 (alveolar epithelial cells) [Fig. S2(d)]. Deletion of ORF23 did not affect lytic virus replication in NIH3T3 or in MLE-12 cells.

To analyse lytic growth of the recombinant viruses in mice, C57BL/6 or BALB/c mice were infected intranasally (i.n.) or intraperitoneally (i.p.) with  $1 \times 10^5$  p.f.u. of the indicated

viruses. Virus titres were determined from lung and spleen homogenates by plaque assay on BHK-21 cells at days 6 and 9 after infection, respectively. As shown in Fig. 2(a), deletion of ORF23 did not affect lytic virus replication *in vivo*. Lungs were also analysed at days 3 and 10 after i.n. infection. Similar to day 6, we did not observe significant differences (data not shown). Since we did not observe differences after infection with  $1 \times 10^5$  p.f.u., we performed an additional experiment with a 100-fold lower dose. Five C57BL/6 mice per group (parental virus,  $\Delta 23$  and  $\Delta 23$ R) were infected i.n. with 1000 p.f.u., and virus titres were determined from lung homogenates at day 6 after infection. Again, no differences were observed (data not shown).

To analyse latent infection, mice were infected with  $1 \times 10^5$  p.f.u. as described above. At day 17 ('early latency'), spleens were harvested and single-splenocyte suspensions were

http://vir.sgmjournals.org

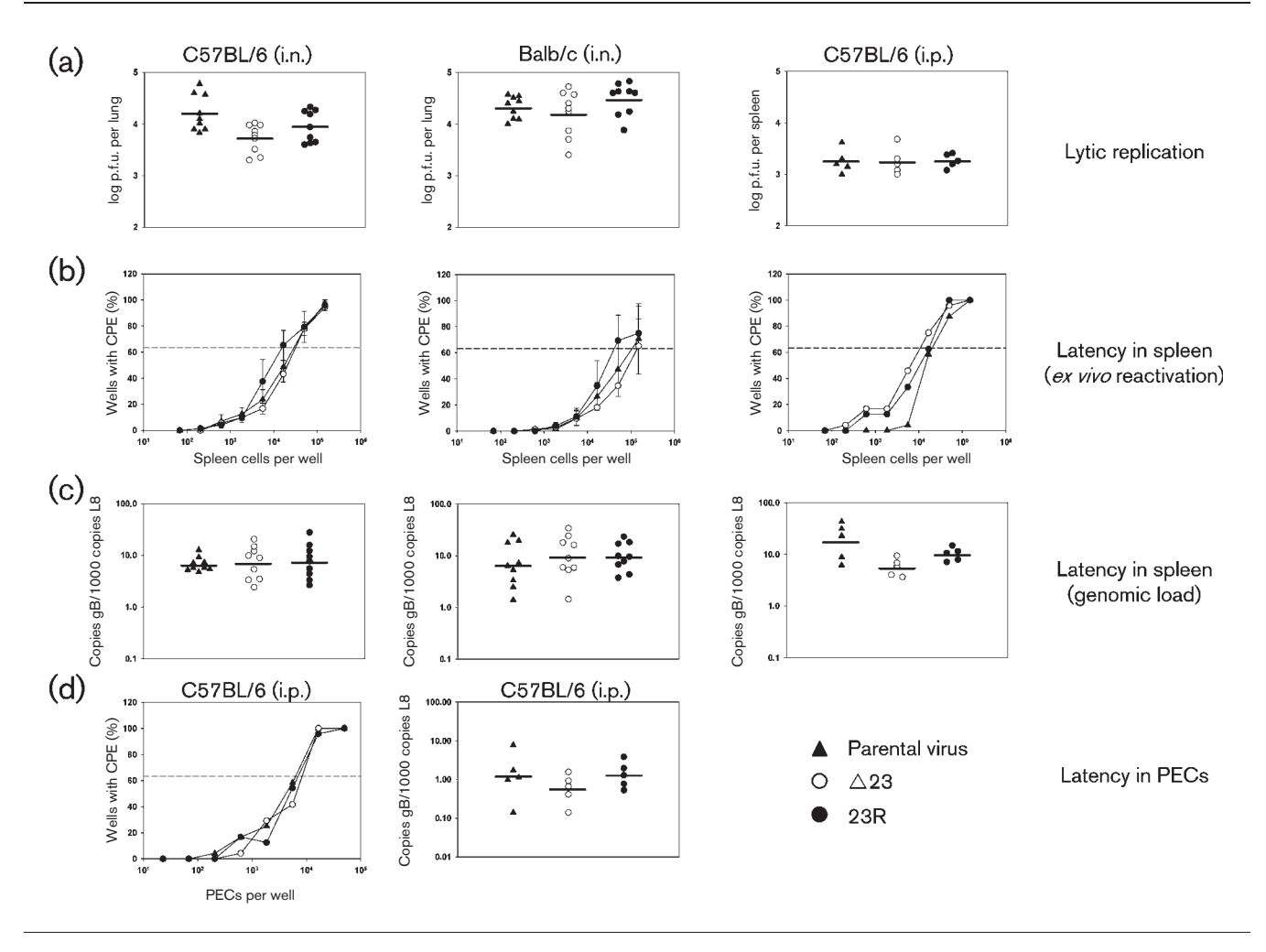


Fig. 2. In vivo growth. (a) Lytic replication. C57BL/6 (left panel) and BALB/c mice (middle panel) were infected i.n. with 1×10<sup>5</sup> p.f.u., or C57BL/6 mice (right panel) were infected i.p. with 1×10<sup>5</sup> p.f.u. of the indicated viruses. Lungs (left and middle panel) or spleens (right panel) were harvested at days 6 (lungs) or 9 (spleens) after infection, and virus titres were determined. Each symbol represents an individual mouse and the bars represent the mean. The data shown in the left and middle panel are compiled from three independent experiments, the data in the right panel are from a single experiment. (b) Latency in spleen (ex vivo reactivation of splenocytes). Mice were infected as described in (a). At day 17, spleens were harvested and singlesplenocyte suspensions were prepared and analysed in an ex vivo reactivation assay. The data shown in the left and middle panel are means ± SEM and are compiled from three independent experiments. In each experiment, splenocytes from three mice per group were pooled. The data in the right panel are from a single experiment with pooled splenocytes from five mice per group. The dashed line indicates the point of 63.2 % Poisson distribution, determined by non-linear regression, which was used to calculate the frequency of cells reactivating lytic replication. (c) Latency in spleen (viral genomic load). Mice were infected as described in (a). At day 17, spleens were harvested and single-splenocyte suspensions were used for DNA isolation for realtime PCR analysis. Each symbol represents an individual mouse and the bars represent the mean. The data shown in the left and middle panel are compiled from three independent experiments, the data in the right panel are from a single experiment. (d) Latency in PECs. C57BL/6 mice were infected i.p. with 1×10<sup>5</sup> p.f.u. of the indicated viruses. PECs were harvested 17 days after infection, and the number of ex vivo reactivating cells (left panel) and the viral genomic load (right panel) were determined. The data in the left panel are from a single experiment with pooled PECs from five mice per group. In the right panel, each symbol represents an individual mouse and the bars represent the mean.

prepared and analysed in an *ex vivo* reactivation assay (Adler *et al.*, 2001). No significant differences were observed (Fig. 2b). We also determined the viral genomic load from the same samples using quantitative real-time PCR (Flach *et al.*, 2009). Again, no significant differences were observed (Fig. 2c). The viral genomic load in the spleen was also analysed at

day 42 ('late latency') after i.n. or i.p. infection. As at day 17, we did not observe significant differences (data not shown). Finally, we analysed latency in peritoneal exudate cells (PECs). C57BL/6 mice were infected i.p., PECs were harvested 17 days after infection and the number of *ex vivo* reactivating cells and the viral genomic load were determined.

As shown in Fig. 2(d), no significant differences were observed. Thus, ORF23 appeared to be dispensable for establishment and maintenance of latency as well as for reactivation from latency at least after infection with  $1 \times 10^5$ p.f.u. Therefore, we again performed an additional experiment with a 100-fold lower dose. Five C57BL/6 mice per group (parental virus,  $\Delta 23$  and 23R) were infected i.n. with 1000 p.f.u., and the number of ex vivo reactivating cells and the viral genomic load were determined 17 days after infection. Again, no differences were observed (data not shown). We also performed a recently established, so-called non-invasive upper respiratory tract (nose) infection (Milho et al., 2009). To this end, we infected five C57BL/6 mice per group and time point i.n. with 1000 p.f.u. of parental virus, Δ23 mutant and revertant without anaesthesia. Lungs were analysed at days 5 and 8 after infection for lytic virus, and spleens were analysed at days 17 and 42 after infection for latent virus by the assays described above. Consistent with a previous report (Milho et al., 2009), infection did not reach the lung, but virus delivered to the nose still established normal persistence in the spleen as determined by quantitative real-time PCR at day 42 after infection. However, again we observed no differences between the groups (data not shown).

So far, using the standard assays, we could neither detect a role of ORF23 during lytic infection nor during latency. However, we hypothesized that the situation might be different if mutant and parental virus are put in direct competition by co-infection. For this purpose, C57BL/6 mice were i.n. co-infected with 1000 p.f.u. of parental virus and additionally of  $\Delta$ 23 mutant. Lungs and spleens were harvested at various time points after infection, and DNA was isolated for real-time PCR analysis by using virus-specific primers to determine the viral load of each virus. In the face of virus competition, the  $\Delta$ 23 mutant showed a moderate but significant reduction both during lytic replication (Fig. 3a; days 3 and 6 after infection) and latency amplification (Fig. 3b; day 17 after infection).

In this study, we investigated the role of ORF23 in the infection cycle of MHV-68. Our analysis of mRNA expression allowed us to classify the ORF23 mRNA as a late transcript, consistent with previous reports (Ahn *et al.*,

2002; Ebrahimi et al., 2003; Johnson et al., 2010; Martinez-Guzman et al., 2003). Cloning of the predicted ORF (Virgin et al., 1997) with an N-terminal FLAG-tag allowed us to express the protein and to analyse its localization in transfected cells. After transient transfection, a protein of the expected size was detectable by Western blotting analysis. In addition, ORF23 protein expression could also be demonstrated by immunofluorescence microscopy. The protein displayed a nuclear localization and was also present in the cytoplasm exhibiting a dotted pattern. Currently, we do not know whether this distribution would be similar during infection or whether it rather reflects an effect of protein overexpression. Simultaneous infection of the transfected cells did not change the staining pattern of the overexpressed protein. Presently, we can only speculate on a possible function of the protein encoded by ORF23. Since ORF23 is transcribed with late kinetics, it is reasonable to assume that it might be a structural protein. For rhesus monkey rhadinovirus, it was shown by mass spectrometry to be virion-associated (O'Connor & Kedes, 2006). However, it was not found in virions of EBV (Johannsen et al., 2004), KSHV (Bechtel et al., 2005) and MHV-68 (Bortz et al., 2003).

The analysis of an ORF23 deletion mutant suggested that ORF23 of MHV-68 is neither essential for replication in cell culture nor for lytic or latent infection in vivo. It is important to highlight that we made our observations after infection of two different mouse strains (C57BL/6 and BALB/c) and by using two different routes of infection (i.n. and i.p.). Furthermore, we analysed two different compartments of lytic replication (lung and spleen) and two different compartments of latency (spleen and PECs). It is known that mouse strain, the route of infection and the compartments analysed may all influence the outcome of an infection with a particular mutant (Barton et al., 2011). A phenotype of the ORF23 deletion mutant, reflected by a moderate reduction in lytic replication and latency amplification, was only detectable when it was, by co-infection, placed in direct competition to the parental virus. There might be several reasons why we did not observe a more pronounced phenotype of the ORF23 deletion mutant: (i) it is possible that deletion of ORF23 alone is not sufficient to

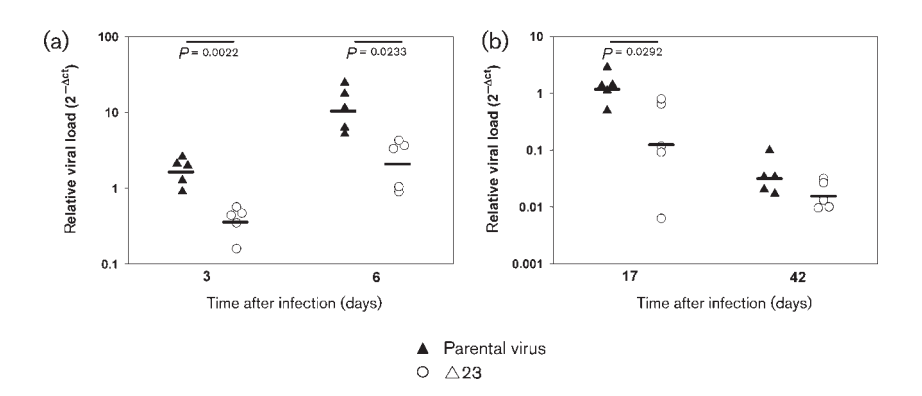


**Fig. 3.** *In vivo* co-infection experiments. C57BL/6 mice were i.n. co-infected with 1000 p.f.u. of each of the indicated viruses. Lungs (left panel) or spleens (right panel) were harvested at the indicated time points and DNA was isolated from the tissues. Real-time PCR analysis with virus-specific primers was performed as described in the Supplementary Methods. Each symbol represents an individual mouse and the bars represent the mean. The data are depicted as relative viral load, and the unpaired Student's *t*-test was used for statistical analysis.

http://vir.sgmjournals.org

generate a phenotype because other viral genes might complement the loss of ORF23; (ii) although ORF23 does not seem to be required for infection in our experimental settings, it might be required for infection parameters we are not able to measure, such as, for example, virus transmission.

Taken together, the precise role of ORF23 during infection remains elusive and further studies will be required to elucidate its function.

## **Acknowledgements**

This work was supported by grants from the BMBF (NGFNplus, FKZ PIM-01GS0802-3) and the Wilhelm Sander-Stiftung (grant no. 2009.046.1) to H. A., and from the Japan Herpesvirus Infections Forum to S. O. We are grateful to the members of our animal facilities for expert technical assistance and to B. Adler for critical reading of the manuscript.

## References

- Adler, H., Messerle, M., Wagner, M. & Koszinowski, U. H. (2000). Cloning and mutagenesis of the murine gammaherpesvirus 68 genome as an infectious bacterial artificial chromosome. *J Virol* 74, 6964–6974.
- **Adler, H., Messerle, M. & Koszinowski, U. H. (2001).** Virus reconstituted from infectious bacterial artificial chromosome (BAC)-cloned murine gammaherpesvirus 68 acquires wild-type properties in vivo only after excision of BAC vector sequences. *J Virol* **75,** 5692–5696.
- Ahn, J. W., Powell, K. L., Kellam, P. & Alber, D. G. (2002). Gammaherpesvirus lytic gene expression as characterized by DNA array. *J Virol* 76, 6244–6256.
- Barton, E., Mandal, P. & Speck, S. H. (2011). Pathogenesis and host control of gammaherpesviruses: lessons from the mouse. *Annu Rev Immunol* 29, 351–397.
- **Bechtel, J. T., Winant, R. C. & Ganem, D. (2005).** Host and viral proteins in the virion of Kaposi's sarcoma-associated herpesvirus. *J Virol* **79**, 4952–4964.
- **Blackman, M. A. & Flaño, E. (2002).** Persistent  $\gamma$ -herpesvirus infections: what can we learn from an experimental mouse model? *J Exp Med* **195**, F29–F32.
- Bortz, E., Whitelegge, J. P., Jia, O., Zhou, Z. H., Stewart, J. P., Wu, T. T. & Sun, R. (2003). Identification of proteins associated with murine gammaherpesvirus 68 virions. *J Virol* 77, 13425–13432.
- Ebrahimi, B., Dutia, B. M., Roberts, K. L., Garcia-Ramirez, J. J., Dickinson, P., Stewart, J. P., Ghazal, P., Roy, D. J. & Nash, A. A.

- (2003). Transcriptome profile of murine gammaherpesvirus-68 lytic infection. *J Gen Virol* 84, 99–109.
- Flach, B., Steer, B., Thakur, N. N., Haas, J. & Adler, H. (2009). The M10 locus of murine gammaherpesvirus 68 contributes to both the lytic and the latent phases of infection. *J Virol* 83, 8163–8172.
- Johannsen, E., Luftig, M., Chase, M. R., Weicksel, S., Cahir-McFarland, E., Illanes, D., Sarracino, D. & Kieff, E. (2004). Proteins of purified Epstein-Barr virus. *Proc Natl Acad Sci U S A* 101, 16286–16291
- Johnson, L. S., Willert, E. K. & Virgin, H. W., IV (2010). Redefining the genetics of murine gammaherpesvirus 68 via transcriptome-based annotation. *Cell Host Microbe* 7, 516–526.
- Martinez-Guzman, D., Rickabaugh, T., Wu, T. T., Brown, H., Cole, S., Song, M. J., Tong, L. & Sun, R. (2003). Transcription program of murine gammaherpesvirus 68. *J Virol* 77, 10488–10503.
- Milho, R., Smith, C. M., Marques, S., Alenquer, M., May, J. S., Gillet, L., Gaspar, M., Efstathiou, S., Simas, J. P. & Stevenson, P. G. (2009). *In vivo* imaging of murid herpesvirus-4 infection. *J Gen Virol* 90, 21–32.
- Nash, A. A., Dutia, B. M., Stewart, J. P. & Davison, A. J. (2001). Natural history of murine  $\gamma$ -herpesvirus infection. *Philos Trans R Soc Lond B Biol Sci* **356**, 569–579.
- Niwa, H., Yamamura, K. & Miyazaki, J. (1991). Efficient selection for high-expression transfectants with a novel eukaryotic vector. *Gene* 108, 193–199.
- O'Connor, C. M. & Kedes, D. H. (2006). Mass spectrometric analyses of purified rhesus monkey rhadinovirus reveal 33 virion-associated proteins. *J Virol* 80, 1574–1583.
- **Simas, J. P. & Efstathiou, S. (1998).** Murine gammaherpesvirus 68: a model for the study of gammaherpesvirus pathogenesis. *Trends Microbiol* **6**, 276–282.
- Song, M. J., Hwang, S., Wong, W. H., Wu, T. T., Lee, S., Liao, H. I. & Sun, R. (2005). Identification of viral genes essential for replication of murine  $\gamma$ -herpesvirus 68 using signature-tagged mutagenesis. *Proc Natl Acad Sci U S A* 102, 3805–3810.
- **Speck, S. H. & Virgin, H. W., IV (1999).** Host and viral genetics of chronic infection: a mouse model of gamma-herpesvirus pathogenesis. *Curr Opin Microbiol* **2**, 403–409.
- **Usherwood, E. J., Stewart, J. P. & Nash, A. A. (1996).** Characterization of tumor cell lines derived from murine gammaherpesvirus-68-infected mice. *J Virol* **70**, 6516–6518.
- **Virgin, H. W., IV & Speck, S. H. (1999).** Unraveling immunity to  $\gamma$ -herpesviruses: a new model for understanding the role of immunity in chronic virus infection. *Curr Opin Immunol* 11, 371–379.
- Virgin, H. W., IV, Latreille, P., Wamsley, P., Hallsworth, K., Weck, K. E., Dal Canto, A. J. & Speck, S. H. (1997). Complete sequence and genomic analysis of murine gammaherpesvirus 68. *J Virol* 71, 5894–5904.

1080